Spatial water surface variations in open channel flows downstream of side disturbances

T. Hosoda, A. Saif & H. T. Puay
Department of Urban Management, Graduate School of Engrg., Kyoto University, Kyoto, Japan

Y. Kouchi
Energia Economic and Technical Research Institute, Chugoku Electric Power Company, Higashi-Hiroshima, Japan

ABSTRACT: This paper deals with the spatial variations of steady open channel flows downstream of an obstacle attached on the side wall of a flume. It is shown theoretically that using the linearized equations of 2-D shallow flows, periodic wavy patterns exist for supercritical flows (Froude number >1), but the amplitude of periodic wavy patterns always attenuates in the downstream direction. Standing waves can exist only for the case of zero friction factor. The attenuation rate increases with the increase of Froude number. These results are verified by hydraulic experiments carried out in this study.

Keywords: Open channel flows, High velocity flow, Water surface profile, Instability

1 INTRODUCTION

The spatial amplification of the sand bars generated downstream of a point bar along a river bend is well known as the over-deepening phenomena of sand bars. Struiksma et al.(1985) formulated this phenomena mathematically, and derived the critical conditions for the spatial amplification of sand bars. Blondeaux & Seminara (1985) derived the analytical solutions on the temporal change of point bars in a sinuous meandering channel. The resonance relation between sinuous channel and bars is included in the solutions. It is well known nowadays that the condition of the spatial amplification of bars by Struiksma et al. (1985) is coincident with the resonance relation by Blondeaux & Seminara (1985). In this paper, we don't deal with the spatial amplification of sand bars but the spatial variations of water surface in steady open channel flows downstream of an obstacle attached on the side wall of a flume.

It is firstly shown theoretically that using the linearized equations of 2-D shallow flows, the periodic wavy patterns can exist for the supercritical flows condition (Froude number >1), but the amplitude of periodic wavy patterns always attenuates downstream direction. The standing waves without attenuation can exist only for the case of zero friction factor. It is also shown that the attenuation rates of periodic wavy patterns increase with the increase of Froude number.

Hosoda & Nishihama (2006) studied the response of water surface to a sinuous open channel and the flow behavior near the resonance condition. Although there is no resonance condition in the case studied in this paper, it is pointed out that if the spatial variations are given on the uniform bottom, the flow can be amplified in the downstream of side disturbances.

Hydraulic experiments are carried out to verify the theoretical findings shown in this paper, changing the hydraulic conditions such as depth, bottom slope, etc.

2 THEORETICAL CONSIDERATIONS

Referring to the coordinate system shown in Figure 1, common plane 2-D shallow flow equations are given by Eqs.(1), (2) and (3).

$$\frac{\partial uh}{\partial x} + \frac{\partial vh}{\partial y} = 0 \tag{1}$$

$$u\frac{\partial u}{\partial x} + v\frac{\partial u}{\partial y} + g\frac{\partial h}{\partial x} = g\sin\theta - \frac{\tau_{bx}}{\rho h} \tag{2}$$

$$u\frac{\partial v}{\partial x} + v\frac{\partial v}{\partial y} + g\frac{\partial h}{\partial y} = \qquad -\frac{\tau_{by}}{\rho h} \tag{3}$$

where (x, y): Cartesian coordinates, (u, v): (x, y) components of depth averaged velocity vectors,

h : depth, θ : bottom slope and (τ_{bx}, τ_{by}) : (x, y) components of bottom shear stress vectors.

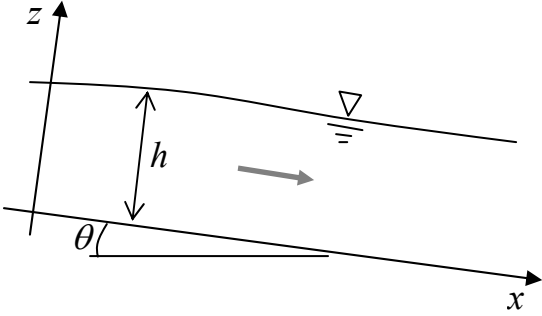For simplicity, the following formula with friction factor, c_f, is applied to evaluate bottom shear stress vectors.

Figure 1 Coordinate system and explanation of symbols

$$\frac{\tau_{bx}}{\rho} = c_f \sqrt{u^2 + v^2}\, u, \quad \frac{\tau_{by}}{\rho} = c_f \sqrt{u^2 + v^2}\, v \qquad (4)$$

Considering the deviation of depth and velocity from the uniform depth and uniform velocity, we can derive the common linearized equations. The uniform depth and uniform velocity in the x direction are given by the following equations:

$$gh_0 \sin\theta = c_f U_0^{\,2}, \quad h_0 U_0 = q \qquad (5)$$

where h_0: uniform depth, U_0: uniform velocity and q: unit width discharge.

Using the following non-dimensional variables with prime, Eqs.(1), (2) and (3) can be transformed into the linearized equations, Eqs.(6), (7) and (8).

$x = Lx', \ y = (B/2)y'$

$h = h_0(1 + \delta h'), \ u = U_0(1 + \delta u'), \ v = U_0 \delta v'$

$$\frac{\partial \delta u'}{\partial x'} + \frac{\partial \delta h'}{\partial x'} + \beta \frac{\partial \delta v'}{\partial y'} = 0 \qquad (6)$$

$$\frac{\partial \delta u'}{\partial x'} + \frac{1}{Fr_0^{\,2}} \frac{\partial \delta h'}{\partial x'} = -\frac{c_f}{\lambda}(2\delta u' - \delta h') \qquad (7)$$

$$\frac{\partial \delta v'}{\partial x'} + \frac{\beta}{Fr_0^{\,2}} \frac{\partial \delta h'}{\partial y'} = -\frac{c_f}{\lambda} \delta v' \qquad (8)$$

where the non-dimensional parameters, β, λ, Fr_0 are defined as follows:

$$\beta = \frac{L}{B/2}, \quad \lambda = \frac{h_0}{L}, \quad Fr_0 = \frac{U_0}{\sqrt{gh_0}}$$

where B: width of channel, L: wave length.

From here, primes indicating non-dimensional variables are omitted for simplicity. Periodic standing wave solutions for small disturbances of depth and velocity components, $\delta h, \delta u, \delta v$ can be written as:

$$\delta h = a_h \sin\left(\frac{\pi}{2}y\right)\cos(2\pi x) \qquad (9)$$

$$\delta u = a_u \sin\left(\frac{\pi}{2}y\right)\cos(2\pi x + \phi_u) \qquad (10)$$

$$\delta v = a_v \cos\left(\frac{\pi}{2}y\right)\cos(2\pi x + \phi_v) \qquad (11)$$

where $\delta h, \delta u, \delta v$ are small increment in h, u, v.

Substituting Eqs. (9)-(10) into Eqs.(6)-(8) yields:

$$2\pi a_u \sin\phi_u + \beta(\pi/2)a_v \cos\phi_v = 0 \qquad (12a)$$

$$-2\pi a_u \cos\phi_u - 2\pi a_h + \beta(\pi/2)a_v \sin\phi_v = 0 \qquad (12b)$$

$$-2\pi a_u \sin\phi_u = -2(c_f/\lambda)a_u \cos\phi_u \\ + (c_f/\lambda)a_h \qquad (13a)$$

$$-2\pi a_u \cos\phi_u - (1/Fr_0^{\,2})2\pi a_h \\ = 2(c_f/\lambda)a_u \sin\phi_u \qquad (13b)$$

$$-2\pi a_v \sin\phi_v + (\beta/Fr_0^{\,2})(\pi/2)a_h \\ = -(c_f/\lambda)a_v \cos\phi_v \qquad (14a)$$

$$-2\pi a_v \cos\phi_v = (c_f/\lambda)a_v \sin\phi_v \qquad (14b)$$

It can be shown easily that Eqs.(12)-(14) have solutions with physical meaning only in the case of $c_f = 0$. The solutions are given by Eqs.(15), (16) and (17).

$$a_u \sin\phi_u = 0, \quad a_u \cos\phi_u = -\frac{a_h}{Fr_0^{\,2}} \qquad (15)$$

$$a_v \sin\phi_v = \frac{\beta a_h}{4Fr_0^{\,2}}, \quad a_v \cos\phi_v = 0 \qquad (16)$$

$$Fr_0^{\,2} = 1 + \frac{\beta^2}{16} \qquad (17)$$

Eq.(17) shows the relation between Froude number of flow and wave length of standing waves. Eq.(17) indicates that the standing waves exist under the condition of super critical flow.

Introducing the spatial functions of amplitudes, $a_h(x), a_u(x), a_v(x)$ in Eqs.(18), (19) and (20), the equations on $a_h(x), a_u(x), a_v(x)$ can be derived as Eqs.(21a,b), (22a,b) and (23a,b).

$$\delta h = a_h(x)\sin\left(\frac{\pi}{2}y\right)\cos(2\pi x) \tag{18}$$

$$\delta u = a_u(x)\sin\left(\frac{\pi}{2}y\right)\cos(2\pi x + \phi_u) \tag{19}$$

$$\delta v = a_v(x)\cos\left(\frac{\pi}{2}y\right)\cos(2\pi x + \phi_v) \tag{20}$$

$$\frac{da_u}{dx}\cos\phi_u - 2\pi a_u\sin\phi_u + \frac{da_h}{dx}$$
$$-\beta\frac{\pi}{2}a_v\cos\phi_v = 0 \tag{21a}$$

$$-\frac{da_u}{dx}\sin\phi_u - 2\pi a_u\cos\phi_u - 2\pi a_h$$
$$+\beta\frac{\pi}{2}a_v\sin\phi_v = 0 \tag{21b}$$

$$\frac{da_u}{dx}\cos\phi_u - 2\pi a_u\sin\phi_u + \frac{1}{Fr_0{}^2}\frac{da_h}{dx} =$$
$$-2\frac{c_f}{\lambda}a_u\cos\phi_u + \frac{c_f}{\lambda}a_h \tag{22a}$$

$$-\frac{da_u}{dx}\sin\phi_u - 2\pi a_u\cos\phi_u + \frac{1}{Fr_0{}^2}2\pi a_h =$$
$$-2\frac{c_f}{\lambda}a_u\sin\phi_u \tag{22b}$$

$$\frac{da_v}{dx}\cos\phi_v - 2\pi a_v\sin\phi_v + \frac{\beta}{Fr_0{}^2}a_h\frac{\pi}{2}$$
$$= -\frac{c_f}{\lambda}a_v\cos\phi_v \tag{23a}$$

$$-\frac{da_v}{dx}\sin\phi_v - 2\pi a_v\cos\phi_v$$
$$= \frac{c_f}{\lambda}a_v\sin\phi_v \tag{23b}$$

We assume Eq.(24) as the mathematical expression of $a_h(x)$, $a_u(x)$ and $a_v(x)$.

$$a_h(x) = A_h\exp(\alpha x), a_u(x) = A_u\exp(\alpha x),$$
$$a_v(x) = A_v\exp(\alpha x) \tag{24}$$

Substituting Eq.(24) into Eqs. (21), (22) and (23), the basic relations on the spatial amplification/attenuation rate, α, and the phase lag between depth variations and velocities can be derived as Eqs.(25), (26), (27) and (28).

$$\cos\phi_u = \frac{P_{\cos\phi u}}{Q_{\cos\phi u}}, \sin\phi_u = \frac{P_{\sin\phi u}}{Q_{\sin\phi u}}, \tag{25}$$

$$\cos\phi_v = \frac{P_{\cos\phi v}}{Q_{\cos\phi v}}, \sin\phi_v = \frac{P_{\sin\phi v}}{Q_{\sin\phi v}} \tag{26}$$

$$P_{\cos\phi u} = \left(\alpha A_u + 2\frac{c_f}{\lambda}A_u\right)\left(-\frac{1}{Fr_0{}^2}\alpha A_h + \frac{c_f}{\lambda}A_h\right)$$
$$-\frac{4\pi^2}{Fr_0{}^2}A_u A_h$$

$$Q_{\cos\phi u} = \left(\alpha A_u + 2\frac{c_f}{\lambda}A_u\right)^2 + 4\pi^2 A_u{}^2$$

$$P_{\sin\phi u} = -2\pi A_u\left(-\frac{1}{Fr_0{}^2}\alpha A_h + \frac{c_f}{\lambda}A_h\right)$$
$$-\frac{2\pi}{Fr_0{}^2}A_h\left(\alpha A_u + 2\frac{c_f}{\lambda}A_u\right)$$

$$Q_{\cos\phi u} = Q_{\sin\phi u}$$

$$P_{\cos\phi v} = -\frac{\beta}{Fr_0{}^2}\frac{\pi}{2}A_h\left(\alpha A_v + \frac{c_f}{\lambda}A_v\right)$$

$$P_{\sin\phi v} = \frac{\beta}{Fr_0{}^2}\pi^2 A_h A_v$$

$$Q_{\cos\phi v} = Q_{\sin\phi v} = \left(\alpha A_v + \frac{c_f}{\lambda}A_v\right)^2 + 4\pi^2 A_v{}^2$$

$$\alpha\frac{\left(\alpha + 2\frac{c_f}{\lambda}\right)\left(-\frac{\alpha}{Fr_0{}^2} + \frac{c_f}{\lambda}\right) - \frac{4\pi^2}{Fr_0{}^2}}{\left(\alpha + 2\frac{c_f}{\lambda}\right)^2 + 4\pi^2}$$

$$+2\pi\frac{2\pi\frac{c_f}{\lambda} + 2\pi\frac{2}{Fr_0{}^2}\frac{c_f}{\lambda}}{\left(\alpha + 2\frac{c_f}{\lambda}\right)^2 + 4\pi^2} + \alpha \tag{27}$$

$$+\beta^2\left(\frac{\pi}{2}\right)^2\frac{\frac{1}{Fr_0{}^2}\left(\alpha + \frac{c_f}{\lambda}\right)}{\left(\alpha + \frac{c_f}{\lambda}\right)^2 + 4\pi^2} = 0$$

$$\alpha\frac{\left(-\frac{\alpha}{Fr_0{}^2} + \frac{c_f}{\lambda}\right) + \frac{1}{Fr_0{}^2}\left(\alpha + 2\frac{c_f}{\lambda}\right)}{\left(\alpha + 2\frac{c_f}{\lambda}\right)^2 + 4\pi^2}$$

$$-\alpha\frac{\left(\alpha+2\dfrac{c_f}{\lambda}\right)\left(-\dfrac{\alpha}{Fr_0^2}+\dfrac{c_f}{\lambda}\right)+\dfrac{4\pi^2}{Fr_0^2}}{\left(\alpha+2\dfrac{c_f}{\lambda}\right)^2+4\pi^2}-1 \qquad (28)$$

$$-\frac{\beta^2}{Fr_0^2}\left(\frac{\pi}{2}\right)^2\frac{1}{\left(\alpha+\dfrac{c_f}{\lambda}\right)^2+4\pi^2}=0$$

Substituting the following functional form, Eqs.(29) and (30) with c_f/λ into Eqs.(27) and (28), the coefficients in these equations can be determined as Eqs.(31) and (32).

$$\alpha=a_0+a_1\left(\frac{c_f}{\lambda}\right) \qquad (29)$$

$$\beta^2=16\left(Fr_0^2-1\right)+b_1\left(\frac{c_f}{\lambda}\right) \qquad (30)$$

$$a_0=0,\quad a_1=-\frac{1}{2}\frac{Fr_0^2+1}{Fr_0^2-1} \qquad (31)$$

$$b_1=0 \qquad (32)$$

Eq.(31) indicates that the spatial disturbances always attenuate in the downstream direction of supercritical flows, and the attenuation rate decreases with the increase of Froude number. Eq.(32) indicates that periodic disturbances can not exist in sub-critical flows.

3 HYDRAULIC EXPERIMENTS

The laboratory tests were carried out to verify the results obtained by theoretical considerations. A schematic illustration of the experimental setup is shown in Figure 2.

As shown in the figure, an obstacle with the shape of the function, $y=A\exp(-Bx^2)$, is attached at 350 cm from the upstream end at the left side wall of the flume. A plot of the obstacle shape is shown in Figure 3.

The hydraulic experiments were conducted to examine the amplification or attenuation of water surface variations in the downstream of the obstacle. Water depth measurements were carried out using point-gauge instrument.

10 cases were performed under different hydraulic conditions. 9 cases were carried under su-

percritical flow condition and one case under sub-critical flow condition. The hydraulic variables for the laboratory tests are listed in Table 1.

Figure 4 shows photographs of flows in Run 1 and 4, while the contour maps of depth are shown in Figure 5.
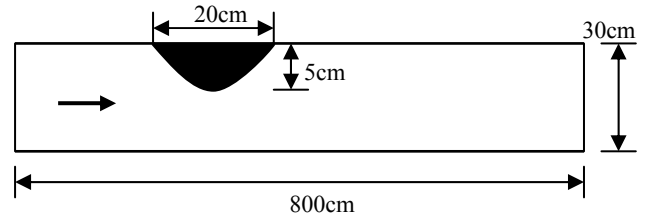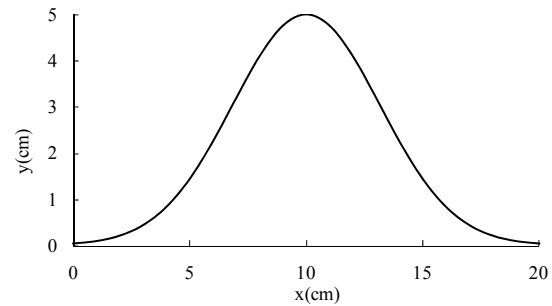
Figure 2 Schematic illustration of flume

Figure 3 Shape function of an obstacle

Table 1 Hydraulic variables of experiments

Run number	Discharge (cm³/s)	Upstream water depth (cm)	Upstream average velocity (cm/s)	Froude number at upstream	Bed slope	Water Temperature (℃)	Flow type
1	6,400	1.74	122.6	2.97	1/34	19.0	Supercritical
2	10,900	2.73	133.1	2.57	1/34	13.5	Supercritical
3	5,950	1.45	136.8	3.63	1/13	19.2	Supercritical
4	7,230	3.15	76.5	1.38	1/156	18.6	Supercritical
5	11,410	3.88	98.0	1.59	1/156	13.2	Supercritical
6	6,620	2.08	106.1	2.35	1/49	13.6	Supercritical
7	11,110	2.96	125.1	2.32	1/49	13.6	Supercritical
8	6,200	2.33	88.7	1.89	1/67	13.2	Supercritical
9	11,200	3.28	113.8	2.01	1/67	13.2	Supercritical
10	7,200	4.46	53.8	0.814	1/326	12.9	Sub-critical

The water surface variations along the both side walls are shown in Figure 6. It is pointed out that the amplitudes of depth variations attenuate in downstream direction for both cases as predicted theoretically in the former section, while we can not identify the magnitude of attenuation rates. It should be noted that since the depth distribution is anti-symmetric, it is necessary to consider the nonlinear effects in the theoretical analysis.

Figure 7 shows the relation between wave length and Froude number for all cases. The solid line in Figure 7 is the linear theory given by Eq.(17). Experimental data are in good agreement with the theoretical curve based on linear analysis, although the nonlinear effect seems to be dominant.
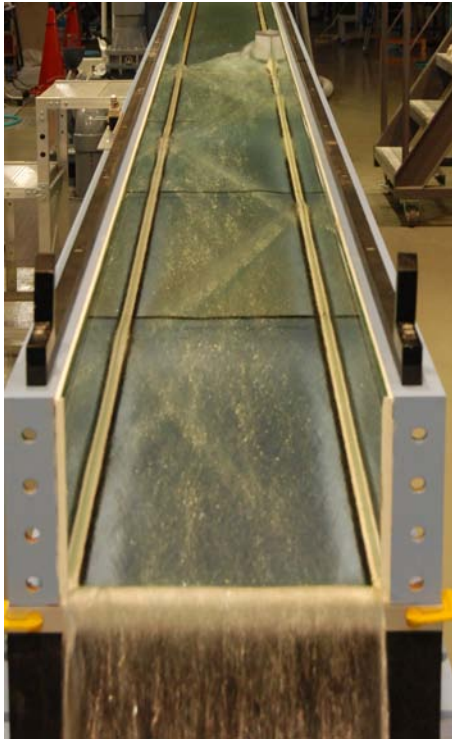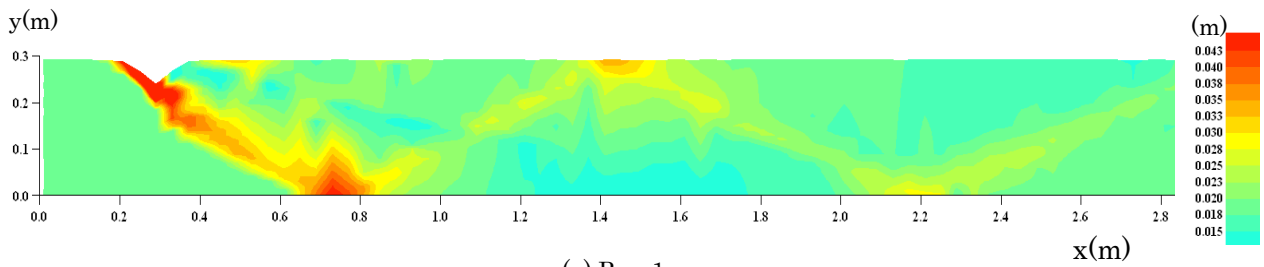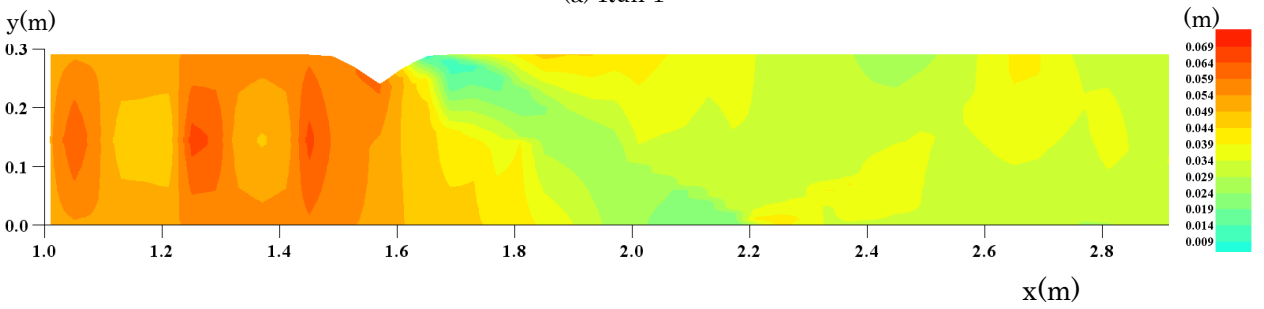
Figure 4 Water surface variation downstream the obstacle (a) Run 1

Figure 4 Water surface variation downstream the obstacle (b) Run 4

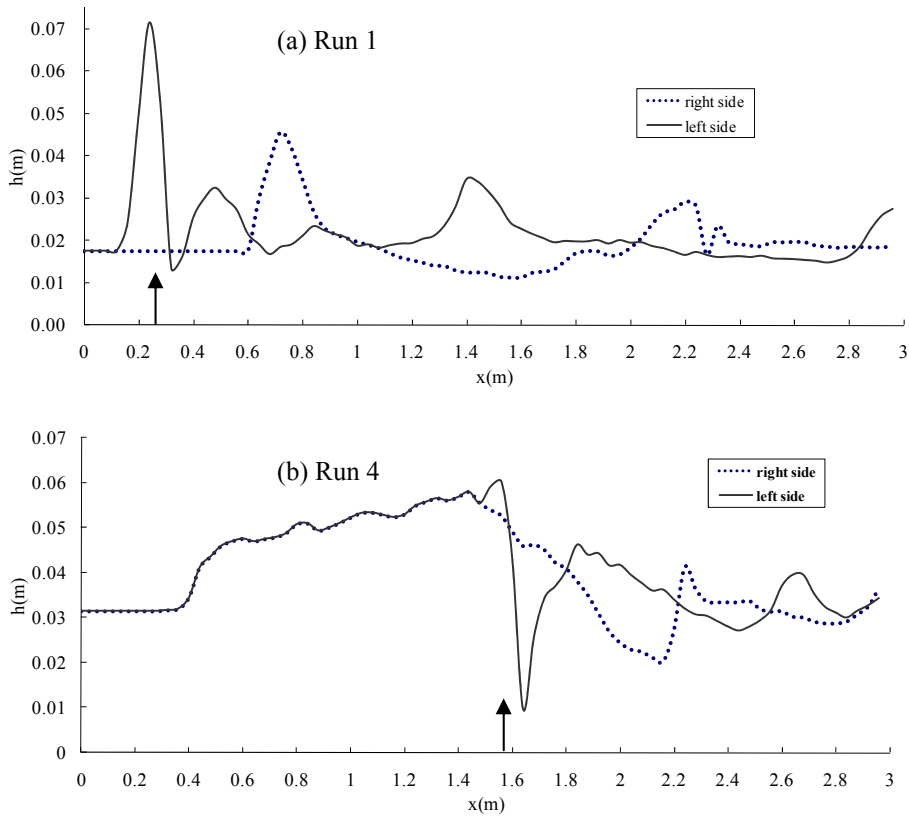(a) Run 1

(b) Run 4

Figure 5 Contour maps of depth
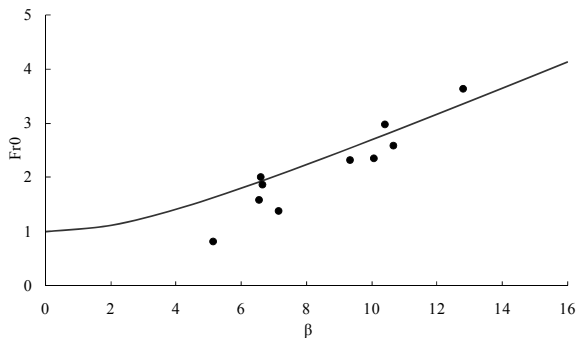
Figure 6 Water surface variations along side wall

Figure 7 Relation between wave length and Froude number

4 CONCLUSIONS

This paper describes the spatial variations of flow depth in steady open channel flows downstream of an obstacle attached on the side wall of a flume. It is shown theoretically that using the linearized equations of 2-D shallow flows, periodic wavy patterns exist for supercritical flows (Froude number >1), but the amplitude of periodic wavy patterns always attenuates downstream direction. The attenuation rate increases with the increase of Froude number.

These results are verified by hydraulic experiments carried out in this study. Since the measured depth distributions show very anti-symmetric feature, the further investigation including the non-linear effects is necessary to clarify the gen-eration mechanism of anti-symmetric depth distributions. Numerical simulation will be also applied to reproduce the flows observed in laboratory tests.

REFERENCES

Struiksma, N., Olesen, K.W., Flokstra, C. and de Vriend, H.J.; Bed deformation in curved alluvial channels, J. of Hydraulic Research, Vol.23, pp.57-79, 1985.

Blondeaux, P. and Seminara, G.; A unified bar-bend theory of river meanders, J. of Fluid Mech., Vol.157, pp.449-470, 1985.

Hosoda, T. and Nishihama, M.; Fundamental characteristics of high velocity flows in a sinuous meandering channel in the vicinity of resonance, River Flow 2006, pp.209-218, 2006.